Journal of Sound and Vibration (1999) **226**(2), 201–216
Article No. jsvi.1999.2273, available online at http://www.idealibrary.com on IDEAL®

THE IMPORTANCE OF SOURCE TYPE ON THE ASSESSMENT OF NOISE BARRIERS

P. JEAN, J. DEFRANCE AND Y. GABILLET

Centre Scientifique et Technique du Bâtiment, 24 *rue Joseph Fourier*, 38400 *Saint-Martin-d'Hères*, *France*

(*Received* 13 *July* 1998, *and in final form* 15 *February* 1999)

A two-dimensional (2-D) boundary element method is used to compute the efficiency of noise barriers in attenuating traffic noise. Different types of source are considered. Point sources and incoherent line sources can be introduced as results of a post-treatment of the 2-D pressure field. The insertion loss of barriers is significantly reduced in the case of more realistic incoherent line sources, as compared to that of coherent line sources. However, the relative efficiency of tops added to a straight barrier is higher.

1. INTRODUCTION

In order to study noise barriers of complex shapes and to assess their efficiency, precise prediction models are required. For instance, geometrical approaches cannot deal with complex diffraction effects. Boundary element techniques [1] are well adapted to this problem, and two-dimensional (2-D) models allow the analysis to be carried out for the full frequency range of interest. In the case of traffic noise, computations must be done up to the 4000 Hz octave band; this cannot be achieved with a 3-D model, whatever the length of the barrier.

Assuming a 2-D problem implies that both the geometry and the excitation are two dimensional; in practice, noise barriers are very long and usually do not vary in cross-section. End diffraction effects are usually negligible. However, the 2-D assumption implies that the sources are infinite in length and coherent. This is not very realistic in the cases of traffic noise or railway noise where the sources, although very long, are rather incoherent. An incoherent line source can be modelled by considering it as a continuous sum of independent point sources.

Recent work by Duhamel [2,3] has shown that it is possible to obtain the pressure field for point sources or incoherent line sources by simply post-processing 2-D results via a fourier-type integration. This technique is used as a means to study the importance of source types when assessing the effectiveness of noise barriers in the case of traffic noise. Summing point sources converges towards the infinite, incoherent line-source result and allows the introduction of air attenuation.

0022-460X/99/370201 + 16 $30.00/0

In order to assess the efficiency of noise barriers, it is important to estimate correctly the total effect of the barrier and the improvement due to modifications, such as the addition of a cap on a straight barrier. The computations confirm the importance of modelling correctly the noise sources in order to assess the absolute and relative efficiency of barriers.

In the work reported here, a variational approach [1] is used to obtain the 2-D solutions. The boundary element program, named MICADO [1], has been adapted for the imaginary-frequency computations necessary to obtain the 3-D solutions [4].

2. THE BOUNDARY ELEMENT PROGRAM

Figure 1 shows the geometry of the 2-D problem, which remains constant along the y-axis parallel to the barrier. The analysis is done for harmonic time dependence $e^{-i\omega t}$. E is an infinite, coherent line source which, therefore, appears as a point source in the 2-D representation. The ground L, along x, is flat, of infinite extent, and may be either rigid or of constant admittance α. A and B are contours, B being above the ground and A being the part of the ground having an admittance different from α.

The theoretical formalism is described fully in reference [1]. It uses the integral representation of the pressure at any point, in terms of the pressure on A and B, the boundary admittances and the elementary Green's solution G. G is the solution for a unit source at Q and an observation point at M when only L is present. It is the sum of three terms

$$G(M, Q) = -(\mathrm{i}/4)H_o(kr) - (\mathrm{i}/4)\, H_0(kr^-) + P_\alpha(M, Q), \tag{1}$$

where r is the (M, Q) distance, r^- is the distance between M and the image of Q with respect to the ground and H_0 is the Hankel function of the first kind and order zero. The second term is the contribution of a hard floor and P_α is the correction factor for ground admittance [5]. P_α is expressed in terms of an integral which, for real frequencies, can easily be computed with a Gauss–Laguerre summation [5].

Since the Green solution includes the infinite ground—hard or absorbent—the integration domain is limited to $A \cup B$. The use of the integral representation and its derivative, combined in a second integration over $A \cup B$, leads to a symmetric

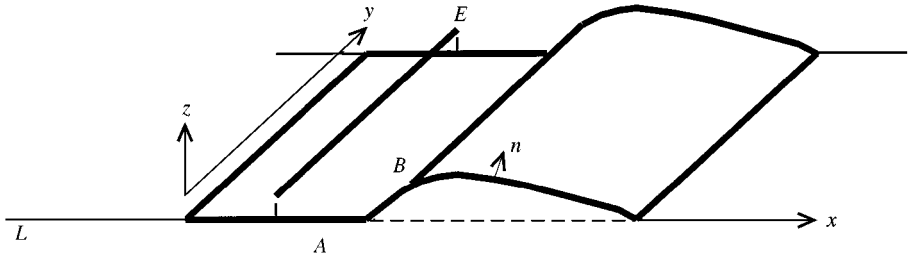

Figure 1. Geometry of the problem: A (on the ground) and B (above the ground) are discretized.

functional in terms of the pressure on the boundaries A and B. A finite-element discretization of A and B, with linear elements, leads to a symmetric matrix.

Several peculiarities of MICADO should be mentioned: the Hankel functions which appear in the elementary Green's terms are tabulated and interpolated when needed, which reduces the computation time required to compute the matrix by a factor of more than 20, without loss of precision; the geometry is defined in terms of segments or portions of circles. At every frequency, adaptive meshing is obtained by dividing each segment into a chosen number of elements per wavelength—typically between three and five elements per wavelength; a Cholevski [6] decomposition of the matrix is used to solve the system of equations. Storing the intermediate decomposition allows several problems for several sources positions to be solved with little increase of computation time. This is particularly important when dealing with several uncorrelated traffic lanes.

3. 2-D TO 3-D TRANSFORMATIONS

3.1. POINT SOURCES

After solving the matrix system, the use of the integral representation of the pressure permits the computation of the acoustical field at any point, in the 2-D situation. Duhamel [2,3] has shown, by using the representation of a 3-D point source in terms of an integral of Hankel functions [7], that it is possible to relate the 3-D pressure field of the 2-D pressure field with the same type of Fourier-like integral:

$$P(x, y, z) = \frac{1}{2\pi} \int_{-\infty}^{\infty} p[x, z, k^*, Z(k^*)\ K/k^*]\ \mathrm{e}^{-\mathrm{i}aY}\ \mathrm{d}a \tag{2}$$

where p is the 2-D pressure at wavenumber k^* and position (x, z), P is the 3-D pressure at wavenumber K and position (x, y, z), $k^* = \sqrt{K^2 - a^2}$, $Y = y - y_S$ where y_S is the y co-ordinate of the point source. $Z(k^*)$ represents the various impedances of the boundaries, including the infinite ground, at wavenumber k^*.

It should be noted that the integrand of equation (2) is a modified 2-D spectrum, the frequency scale being distorted and the impedance spectrum being multiplied by K/k^*. k^* may become imaginary ($a > K$) and the 2-D frequency spectrum necessary to compute the solution at K is limited to k^* which is less than or equal to K ($a = K$, $k^* = 0$). In practice, the imaginary pressure solution decreases very rapidly with frequency and need only be computed for the lower end of the 2-D spectrum—at most up to 100 Hz. In many cases, particularly when A-weighed results are required, they can be omitted. The computation of the 2-D solution for imaginary wavenumbers, when the ground is not rigid, implies the evaluation of the correction term P_α in terms of an integral, for which no simple expression has yet been published and is, therefore, rather computationally time-consuming.

Duhamel [3] introduced the velocity of the sources, since his concern was to estimate precisely the pressure in amplitude and phase in order to study active control of the noise diffracted by noise barriers. However, in order to assess the efficiency of noise barriers, only energy estimates are necessary and the

movement of the vehicles along the road or track does not contribute to the mean energy level.

In order to compute the pressure for 3-D sources—using equations (2) or (3)—the original 2-D spectra must be computed precisely. The well-known problem of irregular frequencies, which is the major drawback of boundary element methods, leads to errors in the solution at frequencies corresponding to the resonance frequencies of the complementary interior problem. Figures 2(a, b) represent the 2-D pressure response for a 1 m wide and 3.05 m high rectangular, rigid obstacle, computed at 1 Hz intervals, first with three elements per wavelength and then with eight elements per wavelength. Figure 2(a) shows a large number of such irregularities, resulting from the somewhat crude meshing of the obstacle. Taking eight elements per wavelength [Figure 2(b)] seem to suppress these irregular frequencies; in fact with five elements per wavelength they almost all disappear. A reduced frequency increment would show that the increase of precision does, in fact, reduce the width and amplitude of the irregular frequencies; thus a meshing of eight elements per wavelength requires a frequency increment of 0.001 Hz to display irregular results of lesser amplitudes. It seems that collocation approaches do not readily avoid problems associated with irregular frequencies [1]; they can give biased results when used to carry out 2-D to 3-D transformations.

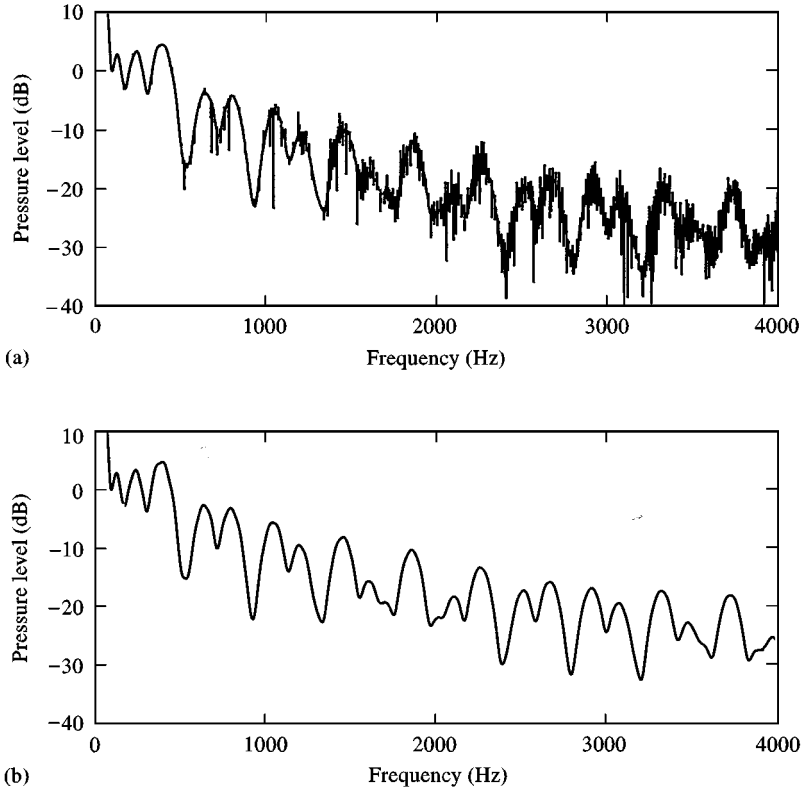

Figure 2. Pressure level referred to level at 100 Hz at point (10.5, 1.5) for a point source at (− 4.5, 1.5). Rigid ground. Rigid rectangular obstacle at $x = 0$ m, 1 m wide and 3.05 m high. (a) meshing with three elements per wavelength (b) eight elements per wavelength.

When all of the boundaries are rigid, the computation of the 2-D spectrum need only be calculated once. However, whenever impedances are introduced, either on the ground or on the obstacle, the modification of the Z spectra by the K/k^* factor implies the need for a full computation of the 2-D solution, up to K, for every K. This could appear to represent an excessive increase in computation time, but as will be seen in the application discussed below, only one frequency per third-octave band suffices in describing the 3-D solution. Finally, the 2-D spectrum should be evaluated starting from very low frequencies at which the computation of P_α is rather expensive, but its precision does not affect the 3-D results. Equation (2) gives the 3-D pressure for an infinite barrier, for a point source and for a point receiver, either of which can be displaced along the noise barrier; oblique incidence effects can therefore be estimated.

3.2. INFINITE, INCOHERENT LINE SOURCES

An incoherent line source is a better approximation for traffic-noise sources since it corresponds to the sum of totally uncorrelated point sources, whereas a coherent line source corresponds to sources emitting in phase. The solution, in the case of an infinite, continuous, incoherent line source, is obtained by integrating an infinite set of uncorrelated point sources. The squared ratio of total pressure to free-field pressure, can be expressed as

$$A(x, y, z) = \frac{1}{2\pi} \int_{-\infty}^{\infty} |p[x, z, k^*, Z(k^*)\ K/k^*]|^2\ \mathrm{d}a \tag{3}$$

Incoherent line sources can be assumed either infinite, equation (3), or comprising a finite length of uncorrelated point sources. Contributions computed using equation (2) are then simply summed in energy.

4. APPLICATION TO TRAFFIC NOISE

The case of traffic noise is now considered. Figure 3 shows a dual-carriageway configuration, with a noise barrier which is 4 m high, at position $x = 0$ m. The four

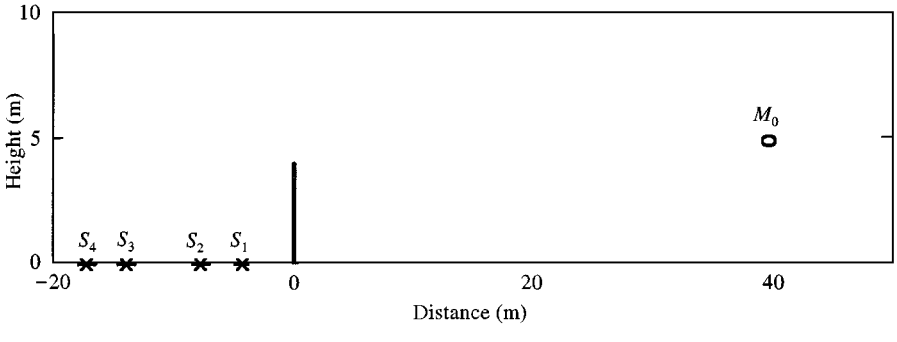

Figure 3. Traffic noise problem. Four lanes S1, S2, S3, S4 at $x = 4.25, -7.75, -14.25, -17.75$, respectively. Receiver point Mo at (40, 5). Three barriers (S, T, C) 4 m high: straight, T-shaped, with cylindrical top.

lanes S1–S4 are positioned at $x = -4.25$, -7.75, -14.25 and -17.75 m, respectively, and unless otherwise stated, are at ground level ($z = 0$ m). The pressure field behind the barrier, between $x = 4$ and 100 m, and between $z = 0$ and 40 m, will be studied. Response spectra are given at Mo = (40,5) m which is a typical point. The noise spectrum of the four independent traffic lanes is given in the European Standard EN 1793-3; the levels in the octave bands 125, 250, 500, 1000, 2000 and 4000 Hz are 86, 90, 93, 96, 93, 88 dB, respectively, with A-weighting corrections included. Three types of barrier–all of the same total height—are considered: a straight barrier; a T-shaped barrier with a 1-m wide top covered with 5 cm of mineral wool; a barrier with a 50-cm wide cylindrical top covered with the same wool (the barriers are referred to as S, T and C, respectively). The mineral wool is characterized by a flow resistivity of $\sigma = 30$ kN s m^{-4} and is described using the Delany and Bazley model [8]. Three cases of ground are considered. First, the ground is considered to be rigid, then it is assumed to be covered with grass ($\sigma = 300$ kN s m^{-4}) and, in the last and most realistic case, the ground under the sources between $x = -20$ and 0 m is assumed rigid in order to represent the asphalt, and is covered with grass elsewhere. The computation time increases by a factor of four between the rigid and grassy ground, and is quite high in the third case where the total surface to be discretized includes 20 m of rigid ground.

4.1. DIFFERENT SOURCE TYPES

Figures 4(a, b) represent the insertion loss (IL) (pressure level without barrier minus pressure level with barrier) of the T barrier at point Mo, for each of the four sources separately and for the four sources together for rigid ground. Figure 4(a) corresponds to the 2-D case (infinite, coherent line sources) and Figure 4(b) to the 3-D case (infinite, incoherent line sources). In both the 2-D and 3-D configurations, the response with the four sources together corresponds to the response of a unique lane situated between lanes S2 and S3, roughly at the mid-position. In the 2-D case, the spread of results between sources is more significant: 6.5 dB(A) compared to 2.5 dB(A) in the 3-D case. Furthermore, the IL is higher: the total IL is 17.9 dB(A) in 2D and 14 dB(A) in 3-D. In the 3-D case, the IL curve is more regular, and the smooth increase with frequency justifies the consideration of only one 3-D frequency per third-octave band, whereas 2-D computations require 30 frequencies per band.

Figure 5 compares the total IL of the four (S1, S2, S3, S4) 2-D and 3-D line sources, and the four point sources facing Mo ($Y = 0$), for the straight barrier and a rigid ground. This result is similar to those of Duhamel [3] obtained for a single source: the IL with point sources is very close to that with infinite, coherent line sources. A lower and smoother IL can be observed for 3-D incoherent line sources.

Figure 6(a) represents—in the case of point source with a straight barrier and a rigid ground–the variation of IL, in dB, as a function of Y (the difference of y positions between point source S1 and receiver Mo), and of the frequency. As Y increases, the interference pattern is shifted towards the higher frequencies, and smaller values of IL are found at the lowest frequencies. Figure 6(b) shows the

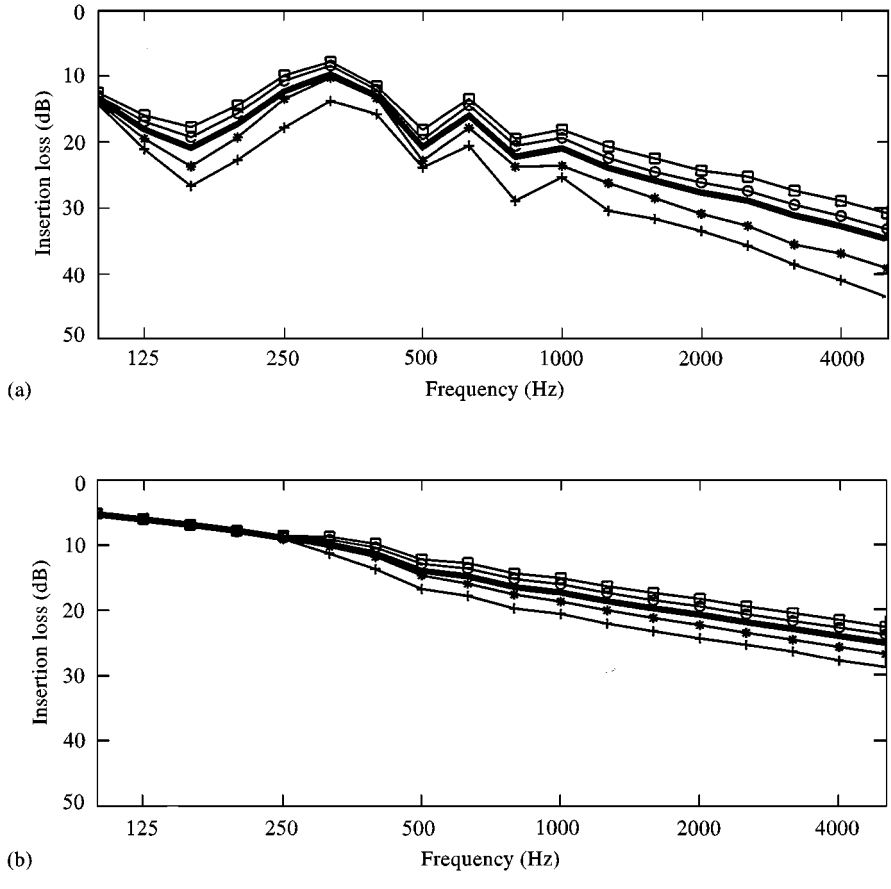

Figure 4. Contribution of the four lanes: S1, S2, S3, S4 (+ , *, ○, □), total (——), T barrier, rigid ground. (a) Coherent lines: dB(A): 22.1, 19, 16.5, 15.6 and 17.9 for total. (b) Incoherent lines: dB(A): 15.3, 14.5, 13.3, 12.8 and 14 for total.

A-weighting integration of IL as a function of Y; lower IL are observed as Y increases.

4.2. AIR ABSORPTION EFFECT

Summing point sources distributed along the barrier gives results which converge towards the infinite, incoherent line source results. Figure 7 compares the values of IL in the case of the straight barrier and a rigid ground, obtained first with a single point source per lane, then with a distribution of 120 point sources per lane positioned regularly between $\theta = \pm 50°$, then with 120 points per lane distributed between $\pm 88°$, and finally in the case of infinite incoherent line sources. For each lane, 2θ is the total aperture, in the horizontal plane, between the point sources and the receiver Mo. The point sources are regularly spaced along θ. Convergence is

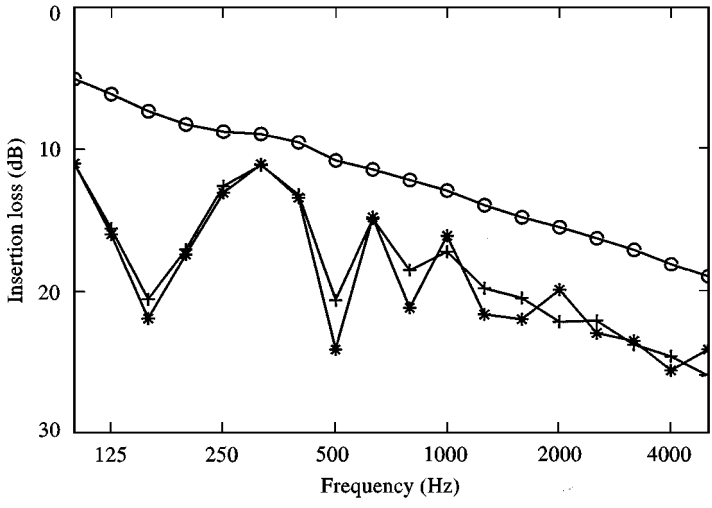

Figure 5. Source-type effect. Straight barrier, rigid ground, +—+ coherent lines: 17 dB(A) *—* point sources: 17.3 dB(A) ○—○ incoherent lines: 11.8 dB(A).

obtained with a wide angular distribution of sources since at the highest frequencies summing up to $\pm 88^\circ$ is not sufficient to obtain the incoherent line source result.

Air-attenuation values of 0.3/0.66/1.57/3.82/9.53/24.2 dB per 1000 m in the octave bands 125/250/500/1000/2000/4000 Hz respectively are introduced. Figure 8 shows that the effect of air absorption is to increase significantly the value of IL at high frequencies in the case of an infinite, incoherent line source.

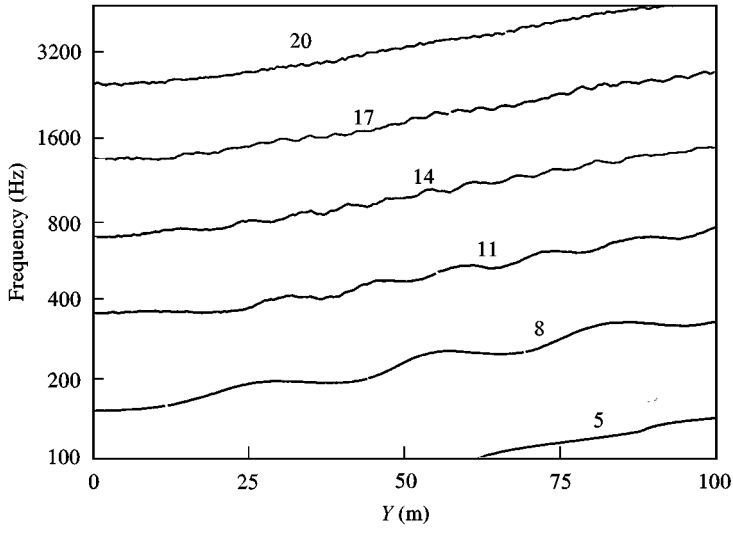

Figure 6(a). Insertion Loss at Mo = (40,0) for a point source S3, when S3 is moved along the barrier: $Y = |y_{S1} - y_{Mo}|$.

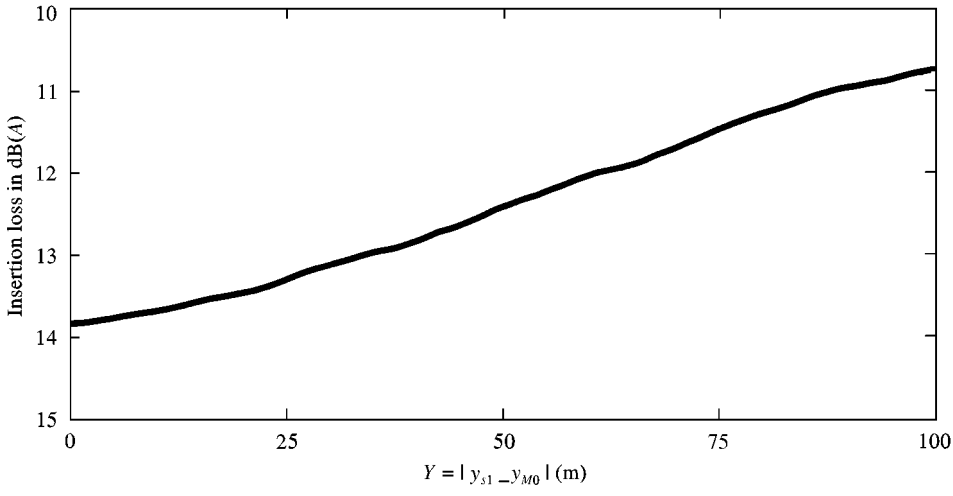

Figure 6(b). Effect of relative y position between point source S3 and receiver at (40,0). Straight barrier, rigid ground.

Table 1 summarizes the effect of air absorption at point (40,0) and (64,10) for the infinite, incoherent line source. The A-weighting values of IL for the three types of barrier and the three types of ground are given without and with air absorption. The effect of air absorption on A-weighting value is significant only with a rigid ground and for the straight barrier, as already shown in Figure 8. The values in the cases of rigid ground and mixed ground are very similar when the absorption of air is considered, implying that it is preferable to use rigid ground than grass in order to approximate the mixed asphalt + grass condition. This result could save

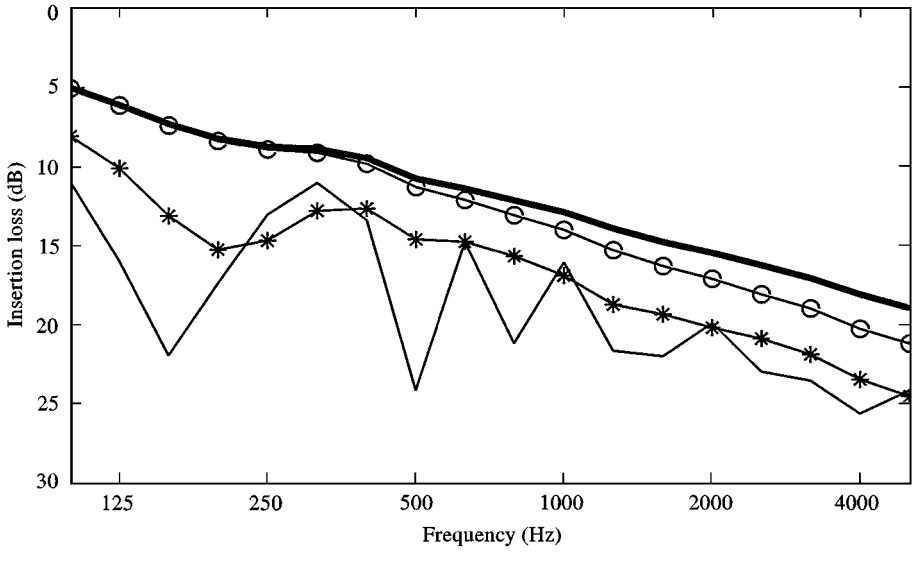

Figure 7. Summation of point sources. Straight barrier, rigid ground. —— one point source per lane facing Mo: 17.3 dB(A), *—* 120 point sources within $\pm$ 50°: 16 dB(A), ○—○ 120 sources within $\pm$ 88°: 12.4 dB(A), —— infinite incoherent line source: 11.8 dB(A).

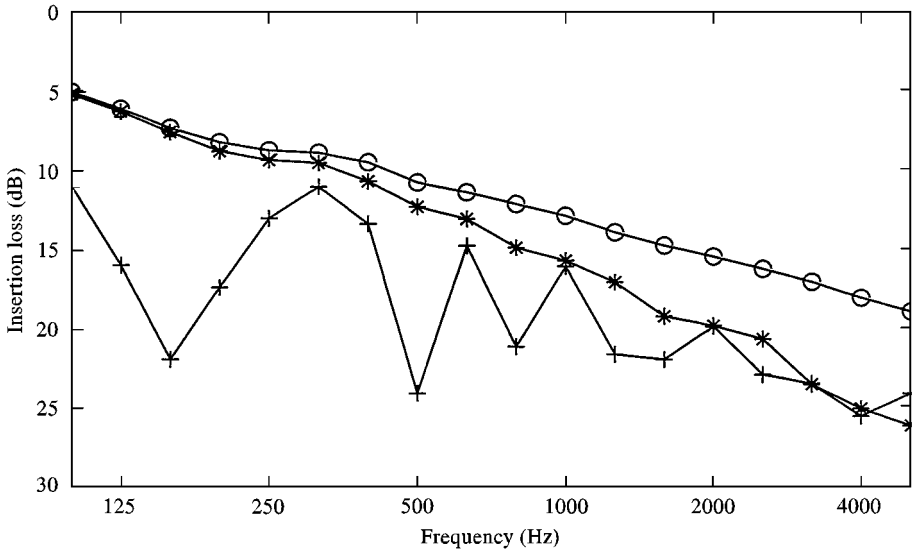

Figure 8. Air absorption effect. Straight barrier, rigid ground. +—+ point sources: 17.3 dB(*A*), *—* incoherent lines with air absorption: 12.9 dB(*A*), ○—○ incoherent lines without air absorption: 11.8 dB(*A*).

computation time, since the addition of 20 m of asphalt to the total boundary multiplies by three the discretized contour and results in a multiplication by nine of the time required to compute the matrices. It has been observed that when the ground is covered with grass, summing point sources between $\pm 75^\circ$ is enough for the calculation to converge towards the infinite line source result, independent of air absorption. When the ground is rigid, the summation must be carried out up to $\pm 88^\circ$ at all frequencies without air absorption; with air absorption, the highest

TABLE 1

Effect of air absorption on Insertion Loss at points (40.5) *and* (68.10).

	Type of barriers					
	S		T		C	
			No air absorption			
Rigid	11·8	11·3	14·0	13·3	13·8	13·1
Grass	10·7	10·5	11·8	11·6	11·4	11·2
Mixed	12·6	12·2	14·6	14·1	15·3	13·7
			With air absorption			
Rigid	12·9	12·4	14·3	13·6	14·0	13·3
Grass	10·7	10·5	11·7	11·5	11·3	11·2
Mixed	12·8	12·5	14·5	14·1	15·0	13·7

Note: S: straight barrier, T-shaped barrier, C: barrier with cylindrical top. Incoherent line source

frequencies will converge for smaller angular aperture. It should be noted that these results depend strongly on the shape of the source spectrum.

4.3. EFFECT OF SOURCE HEIGHT

Figures 9(a, b) compare, for the T barrier and for a rigid ground, the values of IL obtained when the sources are either on the ground or 50 cm above the ground, first for 2-D then for 3-D line sources. The effect of source height is much reduced in the 3-D case and results in small extra oscillations. Recent results by Hamet [9] have shown that, in reality, the equivalent sources associated with traffic are very close to the ground.

4.4. EFFECT OF BARRIER TYPE

Figures 10 (a, b) for 2-D and 3-D line sources, respectively, show the IL for the three types of barriers considered, for a rigid ground. In both cases, the solution

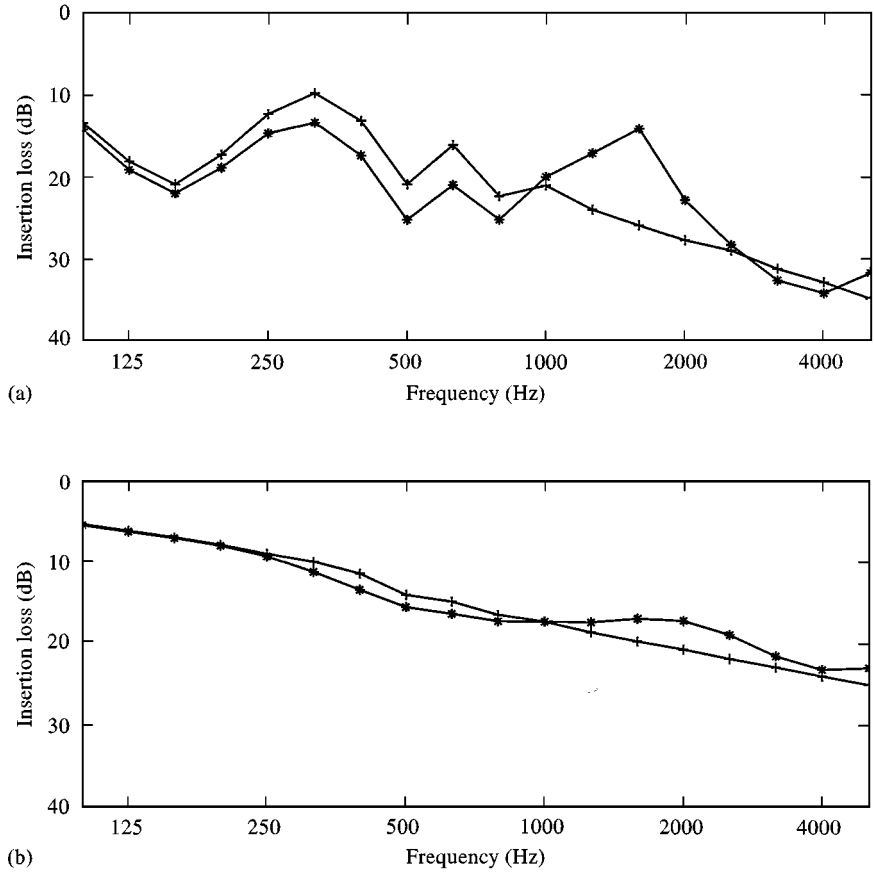

Figure 9. Effect of source height, T barrier, rigid ground, point Mo, +—+ sources on ground, *—* sources 50 cm above ground. (a) Coherent lines, 22.1 and 22.5 dB(*A*); (b) incoherent lines, 15.2 and 14 dB(*A*).

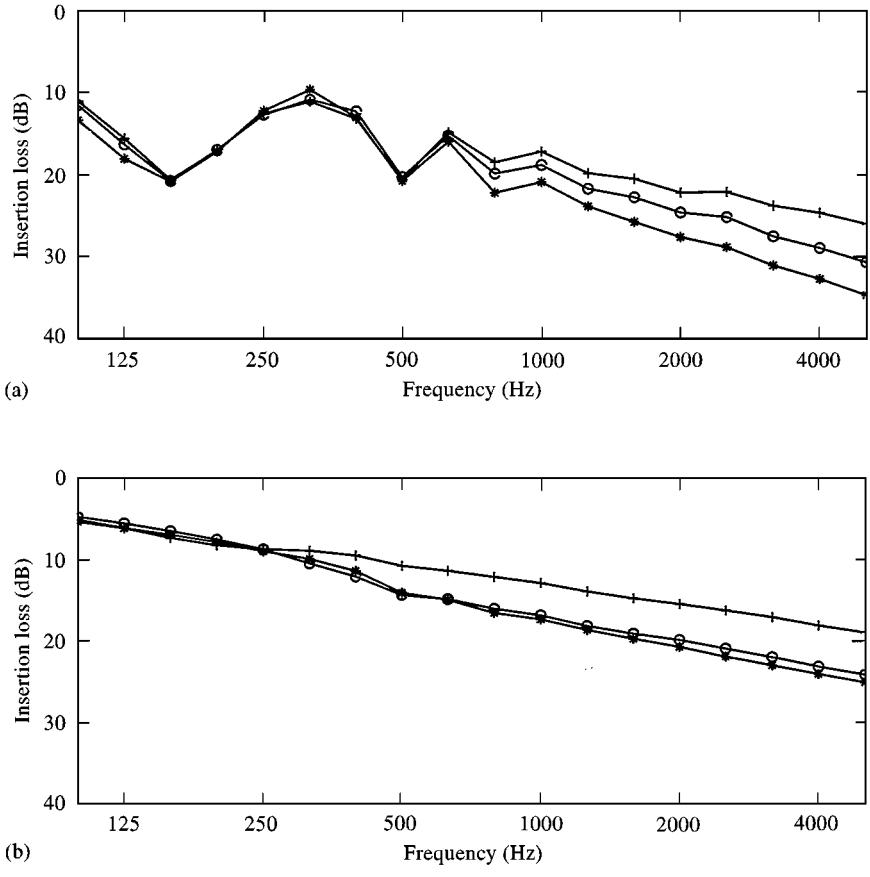

Figure 10. Effect of barrier type, rigid ground, point Mo. +—+ Straight, *—* T barrier, ○—○ cylindrical top: (a) coherent lines, S = 17, T = 17.9, C = 17.5 dB(*A*) (b) incoherent lines, S = 11.8, T = 14, C = 13.8 dB(*A*).

with a cylindrical top is less effective than that of the straight barrier; however, in 3-D the difference between T and C barriers is only 0.2 dB(*A*) and the IL spectra are very similar.

4.5. EFFECT OF GROUND TYPE

Figures 11(a, b) show the effect of ground type in the case of the T barrier. At low frequencies, the IL for the mixed ground (asphalt + grass) is very close to that with grass only. In 2-D, the mixed case will tend towards the rigid case at high frequencies. This is not so in 3-D. As already noted, a very significant increase of computation time is needed to solve the mixed case. Looking at *A*-weighting values (indicated in Table 1 and in the legend of Figure 11) will not permit frequency-dependent effects to be separated; the global indicator obtained for

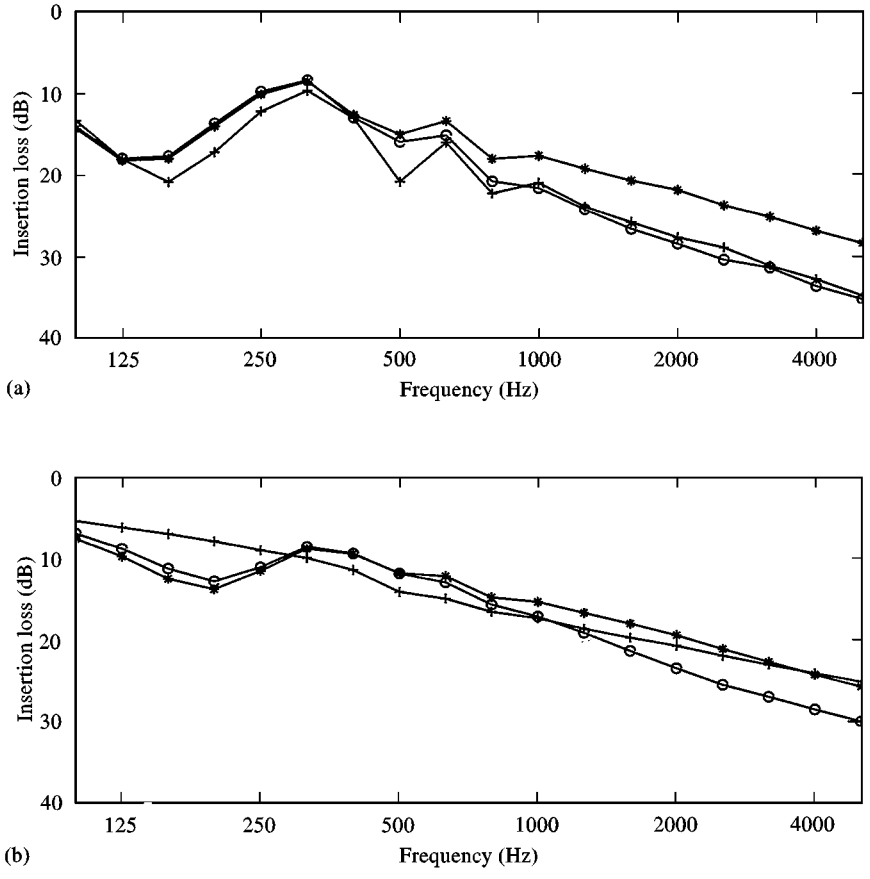

Figure 11. Effect of ground type, T barrier, point Mo. +—+ rigid ground, *—* grass, ○—○ asphalt + grass; (a) coherent lines, rigid = 17.9, grass = 13.8, mixed = 17.4 dB(A) (b) incoherent lines, rigid = 14, grass = 11.8, mixed = 14.5 dB(A).

a given source spectrum shows that the rigid situation is the closest to the mixed-ground case.

4.6. EXCESS ATTENUATION DUE TO T TOP

Figure 12 shows the excess attenuation due to the horizontal top added to a straight barrier for both 2-D and 3-D line sources at point Mo. The global efficiency of the T top is 2.2 dB(A) for the 3-D sources, but only 0.9 dB(A) for the 2-D sources. The middle frequencies are responsible for this increased efficiency in the 3-D case, for this particular source spectrum.

4.7. GLOBAL RESULTS

Figures 13(a, b) represent contour maps of the A-weighting values of IL, for the T barrier and for a mixed ground. The computation points have been taken along

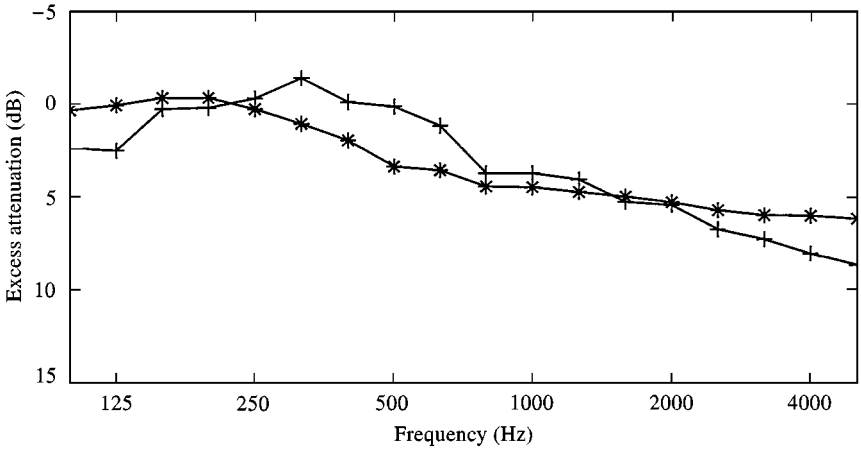

Figure 12. Excess attenuation of the T barrier relative to the straight barrier. +—+ coherent line sources: 0.9 dB(*A*), *—* incoherent line sources: 2.2 dB(*A*). Rigid ground.

the *x*-axis from 4 to 100 m every 14 m, and at heights of $z = 0$, 1, 2, 5 m and then every 5 m up to 40 m. This is a rather rough meshing, but it already leads to a large amount of data to be stored in order to do the 3-D post-processing, since for each barrier, each ground, each source position and each observation point a 2-D spectrum of 1040 frequencies from 0.001 up to 5000 Hz must be considered.

The coherent line source shows values of IL around 14 dB(*A*) near the ground, whereas the more realistic incoherent case shows IL values only around 12 dB(*A*). Figures 14(a, b) represent the relative attenuation of the T top relative to the straight barrier. In 2-D the excess attenuation of the T top lies between 0.5 and 1 dB(*A*), but its between 1.5 and 2 dB(*A*) in the 3-D case.

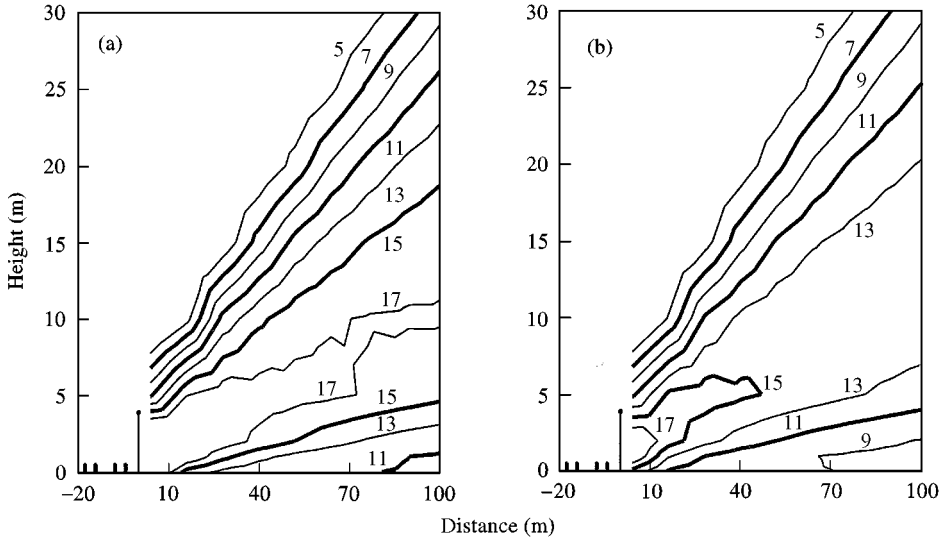

Figure 13. Insertion Loss in dB(*A*) for a T barrier and a mixed ground: (a) coherent lines, (b) incoherent lines.

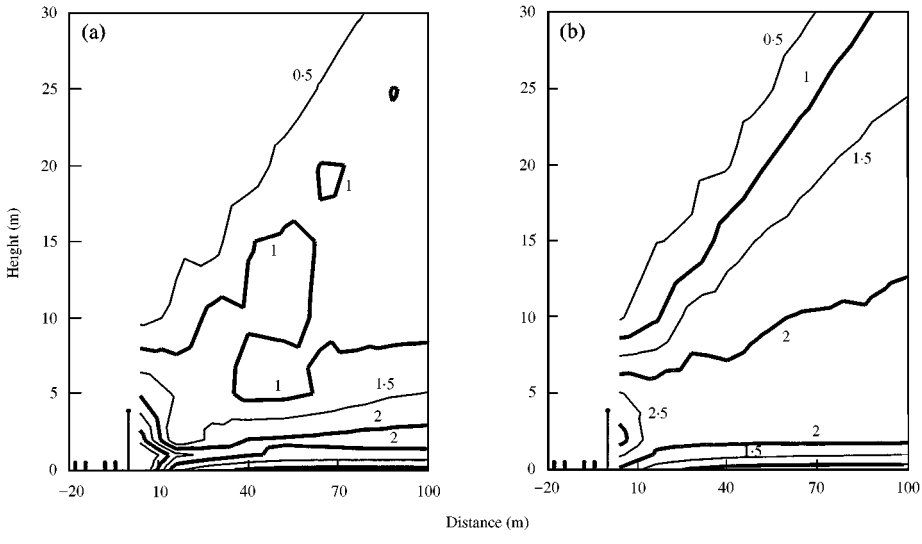

Figure 14. Excess attenuation of T top in dB(*A*), mixed ground: (a) coherent lines, (b) incoherent lines.

Tables 2 and 3 show the mean value of IL between $x = 26$ and 100 m, and between $z = 0$ and 10 m. Results for the three types of barrier and ground are listed. Values in parentheses are the 2-D level minus the 3-D levels indicating the error made by assuming 2-D sources. Most results appear to be ground dependent. For instance, Table 3 shows smaller differences between the 2-D and 3-D excess attenuations (effect of T or C top) if the ground is only covered with grass than for the mixed-ground case.

5. CONCLUSIONS

Boundary-element programs are well suited to the assessment of the effectiveness of noise barriers. In order to make computations up to 5000 Hz, two-dimensional approaches are required. These assume that the geometry is constant, and that the

TABLE 2

Average Insertion Loss in Db(A)

	2-D (2-D to 3-D)			3-D		
	S	T	C	S	T	C
R	15.3 (+ 4·6)	16·6 (+ 3·7)	15·9 (+ 3·3)	10·7	12·9	12·6
G	11·7 (+ 2·1)	12.5 (+ 1·9)	12·0 (+ 1.9)	9·6	10·6	10·1
M	13·6 (+ 3·3)	14.3 (+ 2·4)	13·7 (+ 2·3)	10·3	11·9	11·4

Note: X ∈ [28, 100] *m*, *z* ∈ [0, 10] m. Three types of ground: R (rigid), G (grass), M (mixed) three types of barriers, S: straight, T-shaped, C: with cylindrical top.

TABLE 3

Average gain of top of T and C barrier, relative to straight barrier, in dB(A)

	2-D	(2-D to 3-D)	3-D	
	T/S	C/S	T/S	C/S
R	1·3 (− 1·0)	0·6 (− 1·4)	2·2	1·9
G	0·8 (− 0·2)	0·3 (− 0·2)	1·0	0·5
M	0·7 (− 0·9)	0·1 (− 1·1)	1·6	1·1

Note: $X \in [28, 100]$ *m*, $z \in [0, 10]$ m. Three types of ground: R (rigid), G (grass), M (mixed)

sources are infinite and coherent, along one direction. Noise barriers close to traffic lanes are sufficiently long that they can be considered infinite. However, traffic noise itself is generated by independent vehicles, so each lane must be modelled as an incoherent line source.

Fourier-like transformation allows point sources or incoherent line sources to be considered simply by integrating the 2-D results. In this paper, this transformation is used to quantify the importance of correctly modelling the noise sources. The IL of noise barriers is overestimated if coherent line sources are considered. The effectiveness of a cap added to a straight barrier is underestimated with coherent line sources. Other parameters such as air absorption, the type of ground, the source height, the source and the receiver positions appear to be important when assessing the noise barrier effectiveness.

REFERENCES

1. P. JEAN 1998 *Journal of Sound and Vibration* **212**, 275–294. A variational approach for the study of outdoor sound propagation and application to railway noise.
2. D. DUHAMEL and P. SERGENT Numerical calculation of the three-dimensional sound pressure around noise barriers built over ground of infinite impedance, submitted for publication.
3. D. DUHAMEL 1996 *Journal of Sound and Vibration* **197**, 547–571. Efficient calculation of the three-dimensional sound pressure field around a noise barrier.
4. P. JEAN 1998 *ICA/ASA*, *Seattle*. Source type effect on the efficiency of noise barriers.
5. D. C. HOTHERSALL, S.N. CHANDLER-WILDE and N.N. HAJMIRZAE 1991 *Journal of Sound and Vibration* **146**, 303–322. Efficiency of single noise barriers.
6. W.H. PRESS, S.A. TEUKOLSKY, W.T. WETTERING and B.P. FLANNERY 1994 *Numerical Recipes*. Cambridge: Cambridge University Press.
7. I.S. GRADSHTEYN and I.M. RYZHIK 1980 *Table of Integrals, Series and Products* New York: Academic Press.
8. M.E. DELANY and E.N. BAZLEY 1970 *Applied Acoustics* **3**, 105–116. Acoustical properties of fibrous absorbent materials.
9. J.F. HAMET, M.A. PALLAS, D. GAULIN and M. BERENGIER 1998 *ICA/ASA*, *Seattle*, Acoustic modelling of road vehicles for traffic noise prediction: determination of the sources heights.